

On the origin of lower- and upper-frequency cutoffs on wedge-like spectrograms observed by DEMETER in the midlatitude ionosphere

D.R. Shklyar, Michel Parrot, J. Chum, O. Santolík, E. E. Titova

▶ **To cite this version:**

D.R. Shklyar, Michel Parrot, J. Chum, O. Santolík, E. E. Titova. On the origin of lower- and upper-frequency cutoffs on wedge-like spectrograms observed by DEMETER in the midlatitude ionosphere. Journal of Geophysical Research Space Physics, 2010, 115 (A5), pp.n/a-n/a. 10.1029/2009JA014672 . insu-03035997

HAL Id: insu-03035997

https://insu.hal.science/insu-03035997

Submitted on 2 Dec 2020

HAL is a multi-disciplinary open access archive for the deposit and dissemination of scientific research documents, whether they are published or not. The documents may come from teaching and research institutions in France or abroad, or from public or private research centers.

L'archive ouverte pluridisciplinaire **HAL**, est destinée au dépôt et à la diffusion de documents scientifiques de niveau recherche, publiés ou non, émanant des établissements d'enseignement et de recherche français ou étrangers, des laboratoires publics ou privés.

JOURNAL OF GEOPHYSICAL RESEARCH, VOL. 115, A05203, doi:10.1029/2009JA014672, 2010

Click Here for Full Article

On the origin of lower- and upper-frequency cutoffs on wedge-like spectrograms observed by DEMETER in the midlatitude ionosphere

D. R. Shklyar,[1,2] M. Parrot,[3] J. Chum,[4] O. Santolik,[4,5] and E. E. Titova[6]

Received 22 July 2009; revised 19 November 2009; accepted 5 December 2009; published 7 May 2010.

[1] We report observations of unusual lower and upper cutoff frequencies on VLF spectrograms recorded by the DEMETER satellite (orbiting at ~700 km) during thunderstorm activity. The upper cutoff frequencies in the spectrograms under discussion vary rapidly, approximately in proportion to L^{-3}, where L is the McIlwain parameter on the satellite orbit. On the contrary, the lower cutoff frequencies in the spectrograms are almost constant, so that the cutoffs cross at larger L. Between these cutoffs, which thus form a wedge, intense whistlers are observed, whereas only 0_+ whistlers, and probably, ducted whistlers are present outside the cutoffs. Using a model of lower hybrid resonance (LHR) frequency and local measurements of plasma density and ion composition in the ionosphere, we show that during the events under consideration, the satellite is located at altitudes where the height-dependent variation of the LHR frequency presents a trough. We explain the observed spectrograms on the basis of the features of whistler-mode wave propagation in the inner magnetosphere. Then the upper cutoff frequency is determined by the limiting trajectories that confine the waves of a given frequency propagating obliquely from a source located in the opposite hemisphere. Since the waves close to the limiting ones propagate in the quasiresonance regime, the intensity and time delay at the upper cutoff should increase, which is the case in observations. As for the lower frequency cutoff, it is determined by the LHR maximum, since quasiresonant waves with lower frequencies originating in the opposite hemisphere do not reach the satellite due to the LHR reflection above it.

Citation: Shklyar, D. R., M. Parrot, J. Chum, O. Santolik, and E. E. Titova (2010), On the origin of lower- and upper-frequency cutoffs on wedge-like spectrograms observed by DEMETER in the midlatitude ionosphere, *J. Geophys. Res.*, *115*, A05203, doi:10.1029/2009JA014672.

1. Introduction

[2] The DEMETER satellite is designed to study ionospheric perturbations related to seismic and man-made activity. Its payload consists of wave and particle analyzers. A large part of the electromagnetic (EM) waves recorded by DEMETER consists of whistlers observed at low-latitudes and mid-latitudes, mainly during nighttime [*Parrot et al.*, 2008]. Since the pioneering work by *Storey* [1953] and the classical book by *Helliwell* [1965], a huge number of papers have been published on the generation, the propagation, and the impact of these waves on the ionosphere and the magnetosphere. Still, as thunderstorm activity is one of the most important phenomena in the Earth's atmosphere, much remains to be done to understand all the related effects. The purpose of this paper is to present particular spectrograms of whistlers with lower and upper cutoff frequencies in the VLF range, which are linked to the lower hybrid resonance (LHR).

[3] In the past, *Kimura* [1966] has discovered the role of the LHR in whistler wave reflection, which was first revealed experimentally by *Smith and Angerami* [1968]. *Alekhin and Shklyar* [1980] performed an analytical study of whistler wave propagation in quasiresonance regime and demonstrated a spatial merging of ray trajectories for single frequency waves starting with various initial wave normal angles. *Inan et al.* [1985], when investigating the induced precipitation of radiation belt electrons, revealed the ray trajectory merging for fixed frequency waves injected at different latitudes with vertical wave normal angles. Using INTERKOSMOS-19 data, *Bošková et al.* [1988, 1990a] have shown that LHR whistlers can be detected by satellites moving below the maximum of the LHR frequency height profile, and that they are formed by quasi-electro-

[1]Space Research Institute of Russian Academy of Sciences, Moscow, Russia.
[2]Also at Moscow Institute of Physics and Technology, Moscow, Russia.
[3]LPC2E/CNRS, Orléans, France.
[4]Institute of Atmospheric Physics AS CR, Prague, Czech Republic.
[5]Also at Faculty of Mathematics and Physics, Charles University, Prague, Czech Republic.
[6]Polar Geophysical Institute, Apatity, Russia.

Copyright 2010 by the American Geophysical Union.
0148-0227/10/2009JA014672

static whistler waves propagating in the resonance mode at frequencies near the LHR frequency. A frequency-dependent spatial cutoff of the nonducted ground transmitter signals has been observed experimentally and interpreted theoretically by *Sonwalkar et al.* [1994]. *Shklyar and Jiříček* [2000] and *Shklyar et al.* [2004] used the MAGION 4 and 5 satellite observations of magnetospherically reflected whistlers to perform simulations of the corresponding spectrograms where the LHR reflection is of primary importance. *Chum et al.* [2003] presented oblique noise bands above the local LHR frequency observed onboard the MAGION 5 satellite. They showed that these emissions correspond to nonducted whistler-mode waves of various frequencies propagating near the so-called resonance cone [*Smith and Brice*, 1964]. More recently, using the Radio Plasma Imager on the IMAGE satellite, *Sonwalkar et al.* [2008] classified and identified whistler-mode wave reflection mechanisms, one of them corresponding to the well-known and already mentioned magnetospheric reflection, which takes place at the altitude where the LHR frequency is close to the transmitted pulse frequency. Among hundreds of papers devoted to whistlers we have referred to the above mentioned ones because the results of those papers are closely related to the following consideration, as well as they contain a large number of references to the most important whistler studies. Moreover, the present work can be considered as an extension of the paper by *Walter and Angerami* [1969] who studied nonducted propagation of whistlers between conjugate hemispheres.

[4] The rest of the paper is organized as follows. Section 2 briefly describes the wave experiment onboard DEMETER and presents specific spectrograms with unusual cutoff frequencies. Section 3 contains the discussion of the features of whistler wave propagation in the plasmasphere and the explanation of wedge-like spectrograms. Section 4 gives a summary of the results.

2. Wedge-Like Spectrograms Observed by DEMETER

[5] DEMETER is a low-altitude satellite launched in June 2004 onto a circular polar orbit at the height 710 km. The satellite measures electromagnetic waves all around the Earth except in the auroral zones [*Parrot*, 2006; *Parrot et al.*, 2006]. In December 2005, the altitude of the satellite was decreased to 660 km. The frequency range for the electric field is from DC up to 20 kHz most of which falls into the VLF band. There are two scientific modes of operation: a survey mode where frequency-time spectra of one electric and one magnetic component are computed onboard up to 20 kHz, and a burst mode when, in addition to the onboard computed spectra, waveforms of one electric and one magnetic field component are recorded, permitting spectrum evaluation up to 20 kHz. The burst mode allows a spectral analysis with higher time and frequency resolution. During this mode of operation, the six components of the electromagnetic field are also recorded in the ELF range up to 1.25 kHz, which permits the determination of all wave characteristics, and to perform a wave propagation analysis [*Santolik et al.*, 2003]. Details of the wave experiment onboard DEMETER can be found in the work of *Parrot et al.* [2006] and *Berthelier et al.* [2006a]. The related measurements of ion composition and temperature by the DEMETER thermal plasma analyzer are described by *Berthelier et al.* [2006b].

[6] The figures show wedge-like events recorded by DEMETER. Figure 1 displays a 2 min VLF spectrogram of one electric field component recorded on 3 July 2007 when the instruments operated in the burst mode. The data were recorded in the Southern Hemisphere in the daytime. Low frequency noise can be seen below 500 Hz, but the most intriguing feature is the presence of two distinguished cutoff frequencies between 9 and 15 kHz. The lower one, further called $f1$, is nearly constant during the whole time interval, whereas the upper one, further called $f2$, starts at 14.5 kHz and decreases monotonically, reaching the lower cutoff at 0725:25 UT. Between these two cutoff frequencies, whistler waves are observed. We will identify events which have spectrograms of such type as wedge-like events (WLE). The individual whistler pulses have a special curvature which indicates frequency dispersion during propagation. This curvature is more pronounced close to the upper cutoff frequency $f2$. The shape of the pulses is quite different from that of ducted whistlers, indicating that the former are composed of wave packets traveling along various paths. In the upper part of the spectrogram, signals of VLF ground-based transmitters are observed close to 20 kHz. In the day event shown in Figure 1, the lower cutoff frequency was about 9 kHz, while the wedge ended at $L \simeq 2.9$.

[7] Figure 2 shows the spectrogram of WLE typical of night. The spectrogram was calculated from electric field measurements in the Northern Hemisphere on 6 April 2007. Comparison with the spectrogram in Figure 1 shows that, in the night, WLE are observed at lower L shells ($L < 2.5$) than in the day, and the lower cutoff frequency (~13 kHz) in the night events is essentially higher than in the day ones. (Note that for almost constant altitude of DEMETER, lower L shells imply also lower latitudes.) Other peculiarities that can be observed on the spectrogram are (1) higher spectral intensity near the upper cutoff frequency $f2$, (2) intensification of the spectrum at frequencies corresponding to VLF transmitters, in particular, at $f = 19.8$ kHz, in the L span where the WLE is observed, and (3) absence of low frequencies at lower L shells.

[8] Figure 3 is similar to Figure 1, but the spectrogram is calculated from the data recorded on 2 August 2008. The same cutoff frequencies are clearly seen, although they are not so sharp. In contrast to the spectrogram shown in Figure 1, a series of whistlers in the whole frequency range of the observation can be seen, although some of them suffer attenuation below the lower cutoff frequency $f1$. Their intensities are enhanced between $f1$ and $f2$. This whistler traces also show a more pronounced curvature close to $f2$. Pulses from a Russian VLF ground-based transmitter can be seen between 12 and 15 kHz. These pulses have an increased intensity in the same domain of the spectrogram where the wedge is observed. The spectrograms shown in Figures 1 and 3 were recorded in the daytime when whistlers observed by a satellite are strongly attenuated during their ionospheric propagation [*Fišer et al.*, 2010].

[9] A spectrogram taken in the Northern Hemisphere in the daytime, when the satellite moved toward lower L shells, is shown in Figure 4. In contrast to previous spectrograms, the upper cutoff frequency is now increasing along the

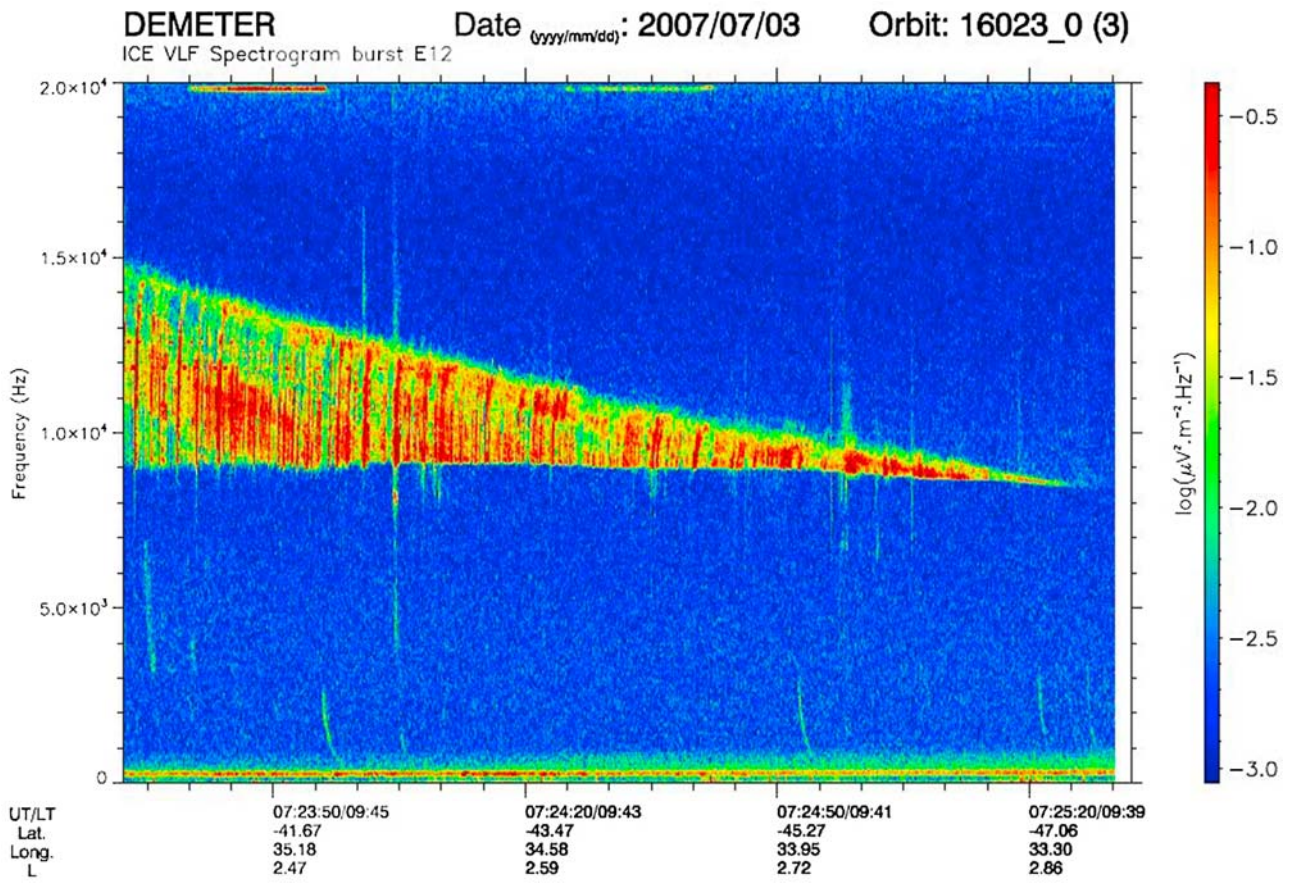


Figure 1. Spectrogram of wedge-like event calculated from electric field measurements in the VLF frequency band up to 20 kHz on 3 July 2007 during local morning. The intensity is color-coded according to the scale on the right. The parameters below the spectrograms indicate universal time (UT), local time (LT), geographic latitude, longitude, and the McIlwain parameter *L*.

satellite path, suggesting that the upper cutoff is connected with the *L* shell of observation. Similar to previous cases, there is an essential increase in VLF transmitter signal intensity on the *L* shell where the transmitter frequency is close to *f*2. While on the spectrograms shown in Figures 2 and 3 the intensification of the spectrum may be due to the addition of a transmitter signal to whistler waves originating from lightning, the intensification of the transmitter signal visible in Figure 4 is most likely due to propagation effects, namely, to trajectory merging (see section 3).

[10] We summarize the observational features of wedge-like events as follows. WLE may be observed in either hemisphere during day and/or night. In the day, the lower cutoff frequency *f*1 is lower than in the night. A similar tendency exists for the behavior of LHR frequency maximum in the upper ionosphere (see Section 3, Figure 9). Since quasi-electrostatic whistler-mode waves suffer magnetospheric reflection from the region where the LHR frequency exceeds the wave frequency, and since DEMETER orbits below the LHR maximum, these suggest that the lower cutoff of WLE (at least of its quasi-electrostatic part) is determined by the LHR maximum. As for the upper cutoff *f*2, the change of its slope depending on the variation of the latitude along the satellite path implies the dependence of *f*2 on the *L* shell of observation. A significant increase of spectral intensity close to *f*2 and the dispersion different from that of ducted whistlers suggest unducted wave propagation with the wave normal angles close to the resonance cone (see Section 3). In the next section we present a detailed quantitative description of WLE formation.

3. Some Features of Whistler Wave Propagation in the Plasmasphere and the Mechanism of Wedge Formation

[11] We assume that the wedge-like spectrograms presented above are formed by whistler waves arising from lightning strokes originating in thunderstorm activity, and that the shape of the frequency-time spectra is determined by a specific location of the satellite (i.e., inside the trough of the LHR frequency profile), and by the features of wave propagation in the nonducted quasiresonance regime. These features have been intensively discussed in the literature. Apart from the already mentioned pioneer and recent studies, we will also refer to the work by *Gendrin* [1961], *Yabroff* [1961], *Smith et al.* [1966], *Walter and Angerami* [1969], *Walker* [1976], *Edgar* [1976], *Alekhin and Shklyar* [1980], *Kimura* [1985], *Bošková et al.* [1990b], *Jiříček*

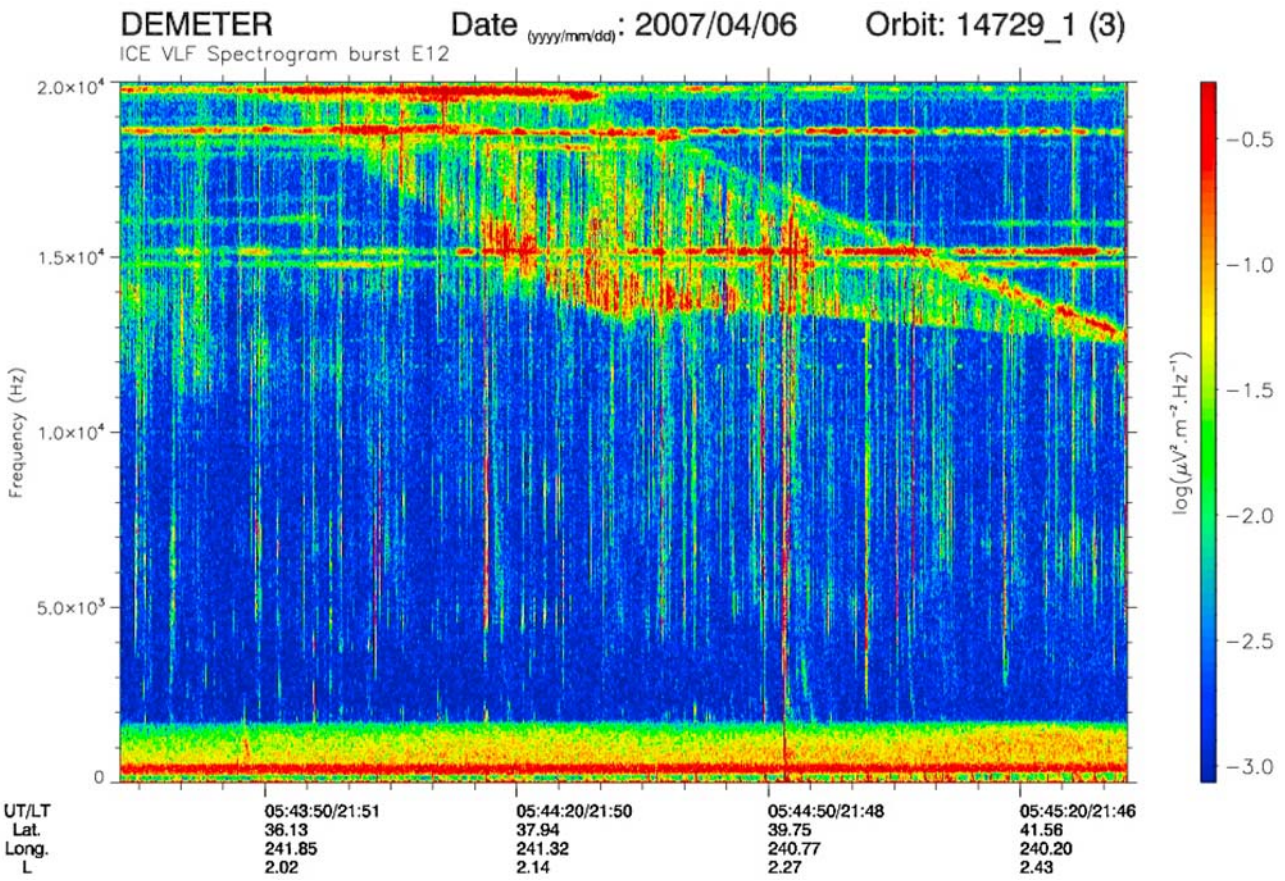


Figure 2. Wedge-like events (WLE) spectrogram recorded on 6 April 2007, during local evening. Signals of several VLF transmitters, which are essentially intensified when WLE is present, are clearly seen.

and Shklyar [1999], *Lauben et al.* [2001], and *Bortnik et al.* [2003a]. Thus, the following summary, which underlines only some features necessary for our consideration, is based on the results of many authors. In particular, *Walter and Angerami* [1969] most closely parallels the present work (see the end of section 3 for specification).

[12] A lightning stroke creates an electromagnetic impulse which gives rise to electromagnetic waves in a wide frequency range, in particular, in the VLF band. These waves start propagating in the Earth-ionosphere waveguide in the form of electromagnetic wave packets. In the course of propagation in the Earth-ionosphere waveguide, the wave energy partly leaks into the ionosphere, and then to the magnetosphere, where it propagates as whistler-mode waves. Owing to the refractive properties of the ionosphere, the wave normal vector for all waves at the entrance point into the ionosphere is almost vertical and thus lies in a meridian plane. In the absence of azimuthal dependence of plasma parameters, which we will assume, the wave vector remains always in the meridian plane, so that wave propagation analysis in 2-D is sufficient. The following consideration originates from the ray tracing in the frame of geometrical optics based on the dispersion relation for whistler-mode waves in a dense plasma, in the frequency range that includes the LHR frequency. This dispersion relation, which can be obtained from the general dispersion equation for a cold magnetized plasma (see, e.g., *Ginzburg and Rukhadze* [1972]), has the form, in standard notation,

$$\omega^2 = \frac{\omega_{\mathrm{LH}}^2}{1 + q^2/k^2} + \frac{\omega_H^2 \cos^2\theta}{(1 + q^2/k^2)^2}\,. \tag{1}$$

Here ω_H is the electron gyrofrequency, the LHR frequency ω_{LH} is determined by

$$\omega_{\mathrm{LH}}^2 = \frac{1}{M_{\mathrm{eff}}} \frac{\omega_p^2 \omega_H^2}{\left(\omega_p^2 + \omega_H^2\right)}; \qquad \frac{1}{M_{\mathrm{eff}}} = \frac{m_e}{n_e} \sum_{\mathrm{ions}} \frac{n_\alpha}{m_\alpha}, \tag{2}$$

where n_e, m_e are electron concentration and mass, respectively, n_α, m_α are the same for ions of species α, k is the magnitude of the wave normal vector, θ is the wave normal angle (i.e., the angle between the wave normal vector and the ambient magnetic field), and

$$q^2 = \omega_p^2/c^2, \tag{3}$$

where ω_p is the electron plasma frequency, and c is the speed of light. Since, at the entrance into the ionosphere $\omega \ll \omega_H$ for all waves in the considered frequency band, and since, not too close to the equator the initial vertical wave normal corresponds to finite cos θ, relation (1) implies that $k^2 \ll q^2$. In this case, which corresponds to the so-called

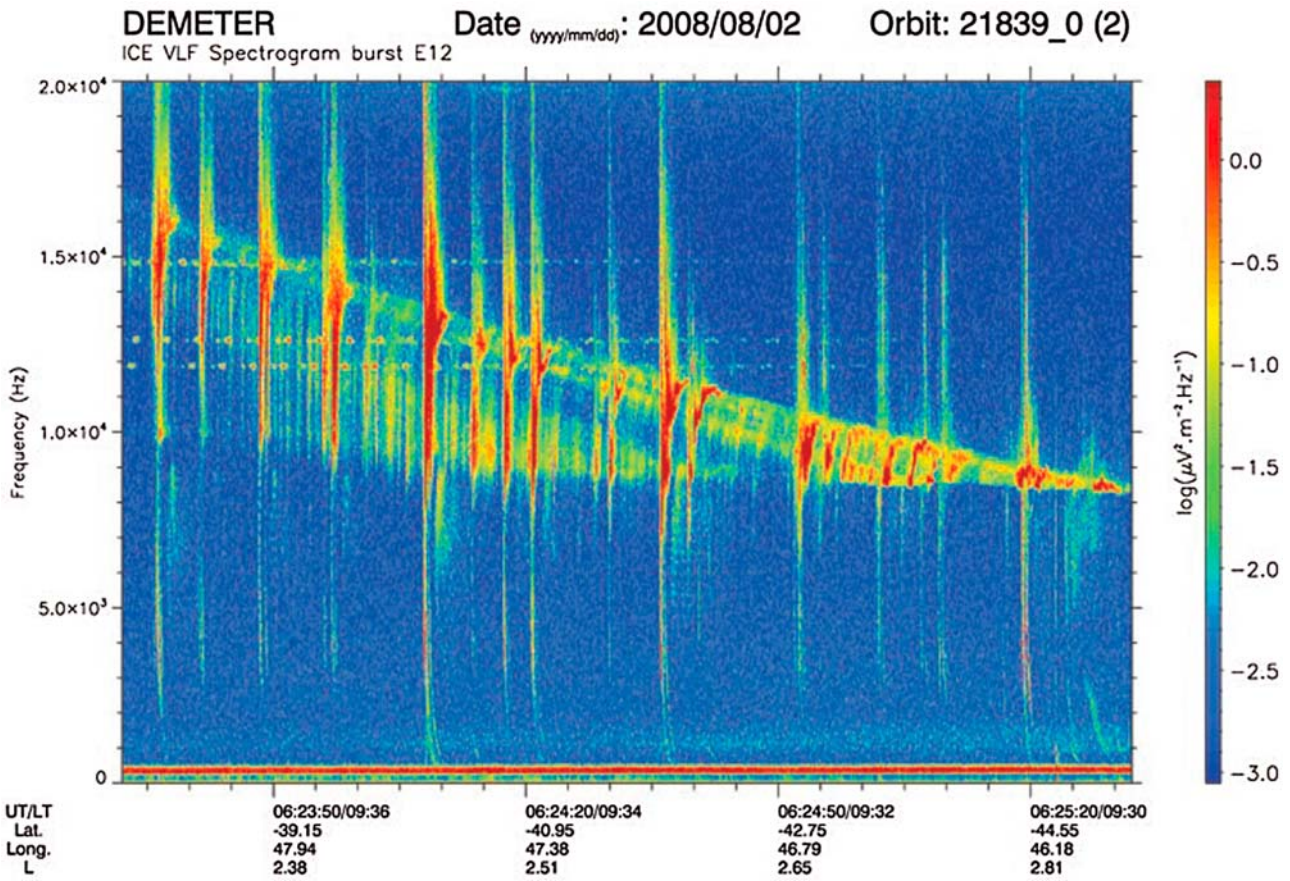


Figure 3. More complex case of WLE emission, complicated by multitude of ducted whistlers, recorded on 2 August 2008 during local morning.

quasilongitudinal electromagnetic waves, the LHR frequency profile does not affect significantly the wave propagation at $\omega \sim \omega_{LH}$, as the first term in (1) is much smaller than the second one. On the contrary, the LHR frequency profile influences the wave propagation at $\omega \sim \omega_{LH}$ most significantly when $k^2 \gg q^2$ and $\theta \rightarrow \pi/2$, which corresponds to the so-called quasiresonance (or quasi-electrostatic) regime of propagation. The transition from the quasilongitudinal to the quasiresonance regime is a well known tendency in nonducted whistler wave propagation in the plasmasphere [*Kimura*, 1985; *Shklyar and Jiříček*, 2000]. As the lower cutoff frequency of the wedge $f1$ is of the order of ω_{LH} in the upper ionosphere, the points mentioned above suggest that the wedge as such is formed by quasiresonance waves coming from the opposite hemisphere, while the general spectrogram may also include 0_+ whistlers and ducted whistlers, of course. Following *Smith and Angerami* [1968], we use the symbol 0_+ and 1_- to denote fractional and full hop whistlers, respectively.

[13] The features of wave propagation from one hemisphere down to ionospheric heights in the conjugate hemisphere are illustrated by Figures 5 and 6. In all cases, the waves are assumed to start at 500 km height with the vertical direction of the wave normal vector. Although the quantitative results of the ray tracing presented below depend on the employed model of plasma parameters, the ambient magnetic field, and the LHR frequency profiles, which are described in detail in the paper by *Shklyar and Jiříček* [2000], the qualitative results do not depend on the model in use. Figure 5 shows the ray trajectories of various frequency waves (from 2 to 20 kHz) starting from the same point and propagating to the satellite height (700 km) in the opposite hemisphere, or to a reflection point. The model LHR frequency used in the ray-tracing calculations depends on altitude and latitude. In the range of L shells from $L = 2$ to $L = 4$, the LHR maximum decreases from 7.9 to 6.3 kHz. We see that 2 and 5 kHz waves are magnetospherically reflected above the satellite height implying that the waves propagate in the quasiresonance regime. Higher frequency waves reach the altitude of 700 km at various L shells, larger frequencies corresponding to lower L shells. This property, which is related to a more pronounced bending toward lower L shells of higher frequency quasiresonance waves, is important for understanding the mechanism of wedge formation. Another important property of VLF wave propagation in the plasmasphere is illustrated by Figure 6, which shows the ray trajectories of 10 kHz waves starting from different latitudes λ_0 in the Northern Hemisphere. Since the frequency is greater than the LHR maximum, all rays reach the satellite height. In general, the final L shell increases with increasing initial λ_0, however, beginning from a certain λ_0 (~43° for 10 kHz waves), all trajectories merge at large latitudes in the Southern Hemisphere so that they cross the satellite height practically at the same L shell. We should

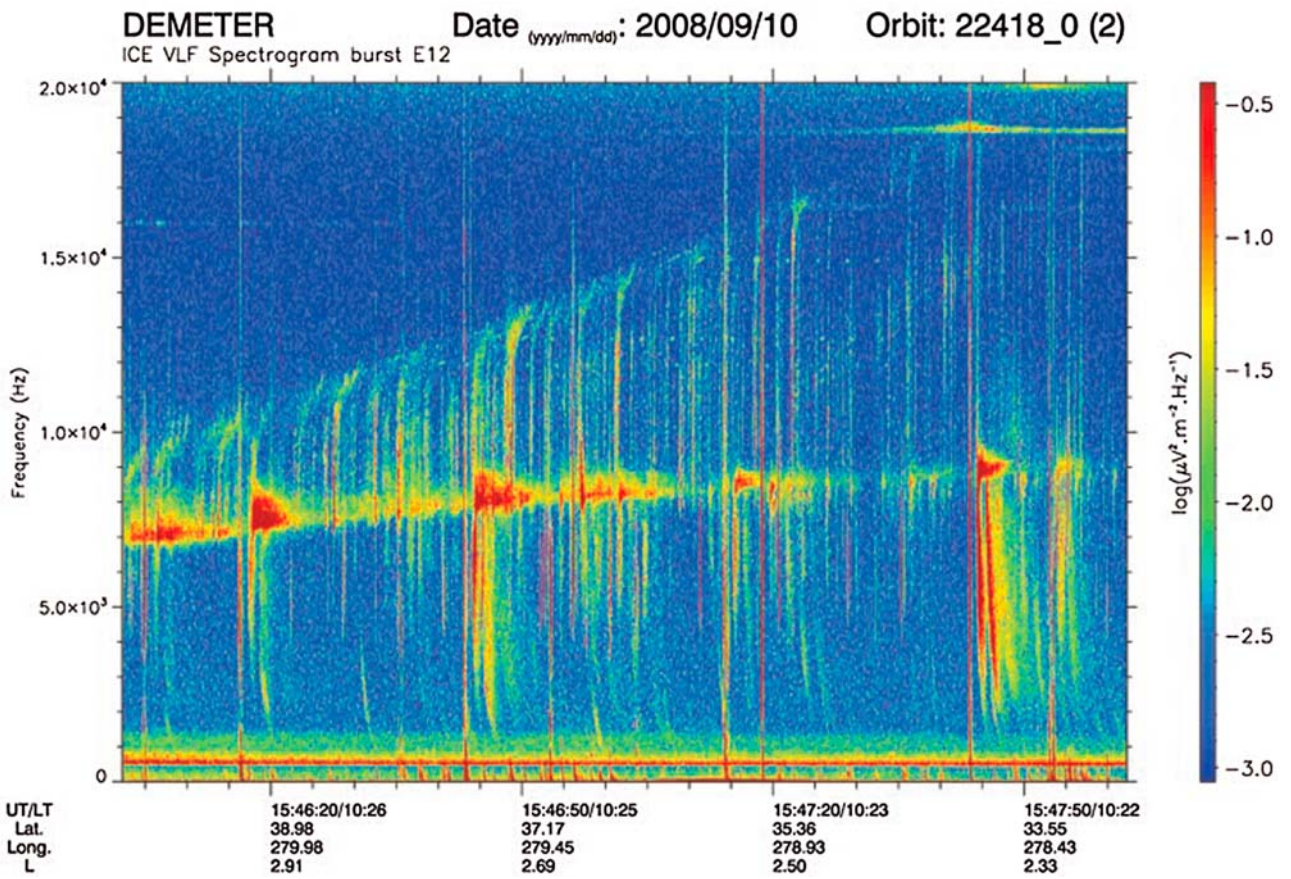


Figure 4. WLE observed on 10 September 2008 around 1025 LT, when the satellite moved toward lower L shells.

underline that, although these rays of the same frequency become more focused at the final L shell, in the absence of sharp density gradients or anomalies, they do not cross each other or form a cusp [*Shklyar and Jiříček*, 2000].

[14] It turns out that the maximum L shell available for a given frequency f above LHR maximum is implicitly described by a simple empirical relation based on ray tracing simulations:

$$f \simeq \frac{f_{H\mathrm{eq}}(L)}{4} \simeq \frac{870}{4L^3}\ \mathrm{kHz}\ , \qquad (4)$$

where $f_{H_{\mathrm{eq}}}$ is the equatorial electron gyrofrequency, and the dipolar model for the Earth's magnetic field has been used. At the same time, relation (4) gives an explicit expression for the maximum frequency which may be observed at low heights on a given L shell, from a source located in the opposite hemisphere and under unducted propagation. According to the first mentioned property of whistler wave propagation in the plasmasphere, all higher frequency waves will reach the satellite height at lower L shells. Although this property of whistler wave propagation has earlier been pointed out by several authors [see, e.g., *Bošková et al.*, 1990b], we show below the results of the corresponding ray-tracing calculations which, along with the relation (4), demonstrate another important property of wave propagation not pointed out earlier. Figure 7 shows the dependence of wave frequency f on the L shell at which it crosses the satellite height (dots) or is reflected above the satellite height (asterisks) for waves starting from various initial latitudes (L shells) in the opposite hemisphere. The curves (from left to right) correspond to initial latitudes (L shells) (a) 35° (L_0 = 1.61), (b) 38° (L_0 = 1.74), (c) 41° (L_0 = 1.89), (d) 44° (L_0 = 2.08), 47° (L_0 = 2.32), 50° (L_0 = 2.61), 53° (L_0 = 2.98), and (e) 56° (L_0 = 3.45), respectively. We remind the reader that, for all waves, the initial height is equal to 500 km. With a very good accuracy, the rightmost curve is approximated by the relation $f = 0.255\, f_{H_{\mathrm{eq}}}(L)$, shown as the solid line in Figure 7. Quite surprisingly, this dependence is valid not only for waves that reach the satellite height, but also for waves which are reflected above the satellite (each frequency reflecting at its own height, of course.) The dotted part of this curve, i.e., the waves which reach the satellite height, defines the highest-frequency observable at the satellite and thus the upper cutoff frequency $f2$ on the spectrograms under discussion. For the model used in the calculations, the maximum of LHR frequency along the field line as the function of L shell is shown in Figure 7 by the dashed line. It is worth noting that the waves at the limiting curve are reflected exactly at the maximum of the LHR frequency profile indicating that they propagate in the resonance regime, while waves starting at lower latitudes penetrate below the LHR maximum, which implies that they propagate in quasilongitudinal mode. We should mention that the wave packets, which undergo magnetospheric LHR reflection above the satellite, never reach the satellite height at a later time.

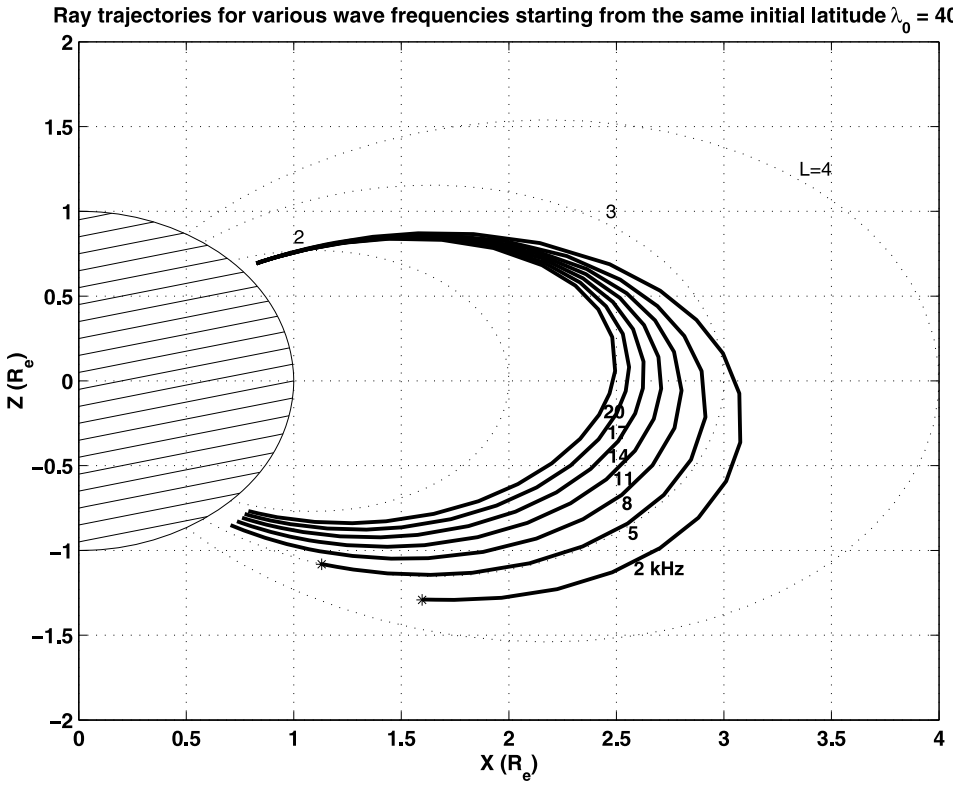


Figure 5. Ray trajectories for 2, 5, 8, 11, 14, 17, and 20 kHz waves. The final L shell at which the wave is either reflected (2 and 5 kHz waves, reflection points marked by asterisks) or reaches the satellite height gradually decreases with the increase of wave frequency.

And the reflections that may take place below the satellite (e.g., reflections from the bottom side of the ionosphere, or reflections due to scattering from small-scale density irregularities) are not included in Figure 7, as those types of reflections are not represented in the frame of geometrical optics (i.e., ray tracing), on the basis of which the pattern in Figure 7 has been calculated. As was mentioned above, most of the features of whistler wave propagation in the plasmasphere which we discussed here have been known from previous work of various authors. Thus, for instance, the raypaths merging into a limiting trajectory and the related frequency-dependent spatial cutoff of the nonducted whistler waves have been previously pointed out by *Walter and Angerami* [1969], *Inan et al.* [1985], and *Sonwalkar et al.* [1994].

[15] Comparison of the observed spectrograms with the ray-tracing calculations, which are summarized in Figure 7, shows that the dependence of the upper cutoff frequency on the L shell along the satellite path is correctly described by the limiting curve in Figure 7. More definitely, we can always choose the maximum latitude of the illuminating region (i.e., the region from which the waves excited by lightning strokes penetrate into the upper ionosphere) so that the corresponding limiting curve approximates correctly the upper cutoff frequency on the WLE spectrogram. This is illustrated by Figure 8, which shows the typical behavior of the upper cutoff frequency in WLE events observed by DEMETER. The dashed lines correspond to two daytime spectrograms represented in Figures 1 and 3. The black (dark) solid lines correspond to nighttime WLE events recorded on 6 April 2007 (Figure 2), 22 September 2006, and 31 March 2006. As was noted above, the lower cutoff frequency for daytime WLE events, which is of the order of 7–9 kHz, is lower than for nighttime events for which it is about 11–14 kHz. As the minimum upper cutoff frequency corresponds to the wedge spike where the lower and upper cutoffs are equal, this minimum upper cutoff for daytime WLE events appears to be lower than for nighttime ones. The utmost solid grey line and the utmost line drawn in small grey squares represent the dependence of the upper cutoff $f2$ on L calculated under assumptions that the maximum latitude of the illuminating span is equal to 56° and 40°, respectively. One can see that, in all cases presented in the figure, the variation of the upper cutoff frequency is similar to L^{-3}, in agreement with the calculated dependence (see Figure 7).

[16] Concerning VLF transmitter signals, they are subject to all the propagation features described above. Thus, their intensity should have a pronounced maximum on the L shells determined by (4) (under appropriate positional relationship between transmitter and receiver, of course) in a good agreement with the experimental data.

[17] As for the lower cutoff frequency, it cannot be directly inferred from the pattern in Figure 7 as the latter includes only 1– whistlers, but does not take into account wave scattering or reflection of any type. Thus, a more comprehensive consideration is needed for understanding the origin of the lower cutoff frequency. In this connection we remember that, at $L \sim 2.5$–3, the characteristic time between two successive LHR reflections is of the order of seconds,

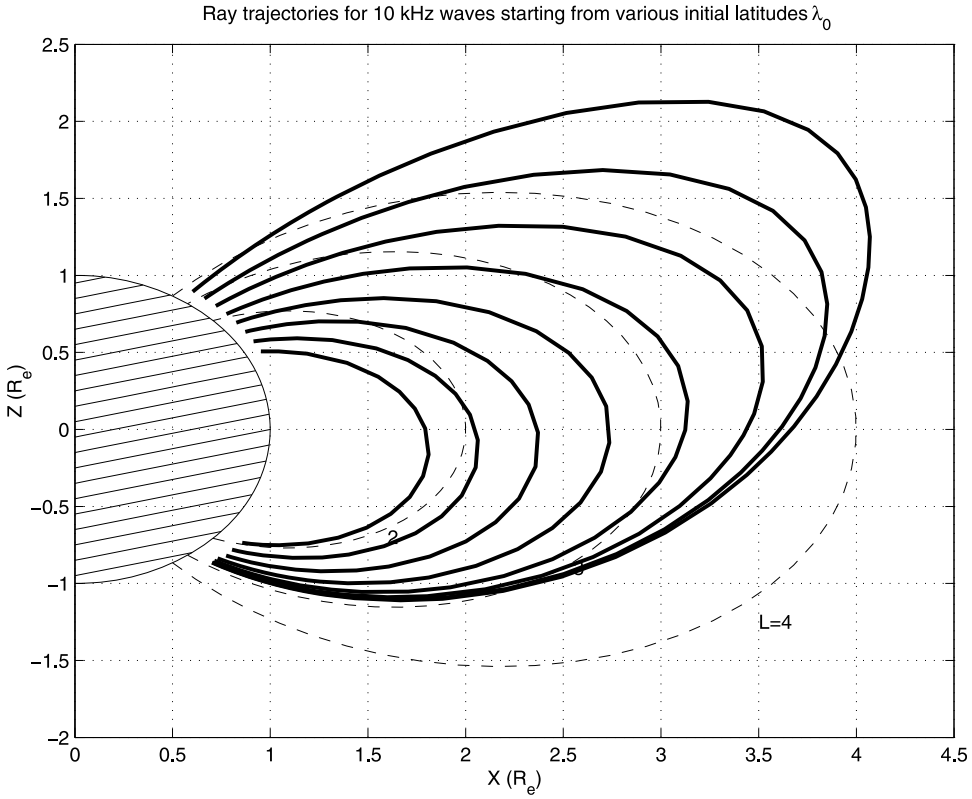


Figure 6. Ray trajectories toward the satellite heights for 10 kHz waves starting in the Northern Hemisphere at 500 km height. Initial latitudes λ_0 are from 28° to 56°. Satellite moving at 700 km height in the Southern Hemisphere, over the line where the trajectories end, observes the so-called 1_ whistler waves. The same applies to trajectories, which reach the satellite height, shown in Figure 5.

and that a wave packet may survive quite a few bounce periods related to these reflections. A typical number of bounce oscillations of magnetospherically reflecting (MR) whistlers observed experimentally is of the order of 5–7 [see, e.g., *Smith and Angerami*, 1968; *Shklyar et al.*, 2004] which corresponds to time ~10 s that agrees well with a theoretical estimation of the lifetime of MR whistlers under the assumption that it is determined by Landau damping [*Bortnik et al.*, 2003b]. Magnetospheric reflection of a whistler-mode wave implies the quasiresonance regime of propagation, which becomes progressively prevalent with the increasing number of MR whistler bounce oscillations in the plasmasphere. Since a typical time of whistler propagation in quasiresonance regime is significantly larger than the time of propagation in quasilongitudinal regime, overview spectrograms which represent ~2 min of wave measurements should be dominated by quasiresonance waves, which only propagate provided that $f > f_{LH}$. Since the group velocity of quasiresonance LHR waves is virtually parallel to the ambient magnetic field, the maximum of LHR frequency along a given field line L should coincide with the lower cutoff frequency on the spectrogram taken at this L shell. Typical LHR frequency profiles, i.e., the LHR frequency (x axis) as the function of height (y axis) on a given field line L, are shown in Figure 9. The left and right panels give the profiles typical of day and night, respectively. The calculated profiles are based on the Truhlik, Triskova, Smilauer (TTS) model of relative ion densities and electron density in the topside ionosphere. This model is a part of the international reference ionosphere (IRI) and is described by *Triskova et al.* [2003], *Truhlik et al.* [2004], and *Triskova et al.* [2006]. We see that the LHR maximum in the daytime is smaller than in the nighttime, as well as the lower cutoff frequency on spectrograms in the daytime is smaller than in the nighttime, although the absolute values of LHR maxima and lower cutoff frequencies differ appreciably. Though there are cases in which the lower frequency cutoff is very close to the maximum of LHR frequency.

[18] As was mentioned above, the lower cutoff frequency obtained in the simulations depends on the plasma density, ion composition, and magnetic field model used in the ray tracing. In order to verify the robustness of our results, we also used another ray-tracing procedure based on full cold plasma dispersion relation, International Geomagnetic Reference Field (IGRF) model for magnetic field, and diffusive equilibrium for the ion composition in the upper atmosphere, all taken for one particular case of a WLE event (specified further in this section). This version of the ray tracing, described by *Cerisier* [1970] and *Cairo and Lefeuvre* [1986], was substantially modified and used by *Santolik et al.* [2009] to study the propagation of the nonducted whistlers from their source. *Chum et al.* [2009] used this ray tracing in their investigation of subprotonospheric whistlers observed by DEMETER. In our study, we fitted the ion composition and the plasma density to the values given by IRI2007 model at the location of DEMETER at 0724:00 UT on 3 July 2007. This means that the obtained

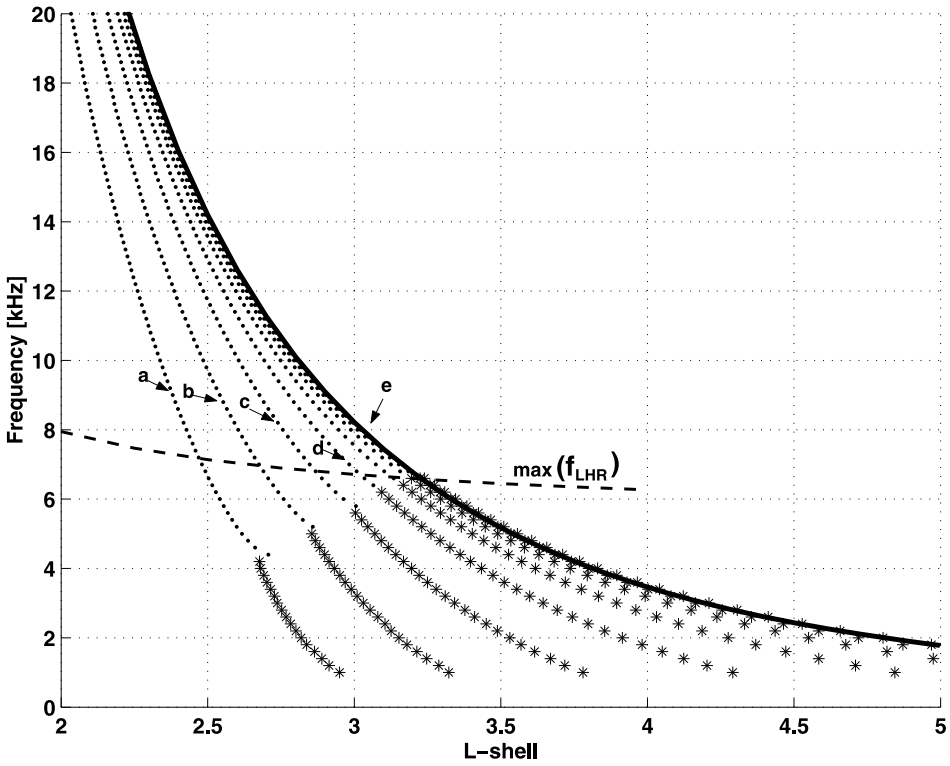


Figure 7. ($L - f$)-plane defining expected frequency cutoffs $f2$ (see the text for details).

results can be related to the observation presented in Figure 1. Since we used the IGRF magnetic field model, the ray tracing was run in geographical coordinates. The initial geographical latitudes were 36°N, 42°N, 47°N, 51°N, and 58°N. The results obtained are displayed in Figure 10. Because of the time demands for calculations, we used a 0.5 kHz step-in frequency. Otherwise, the meaning of the lines and symbols is the same as in Figure 7, i.e., the wave packets that reach the satellite height and are reflected above it are shown by dots and stars, respectively, and the value of the maximum of LHR frequency is indicated by a dark dashed line. In addition, the height of this maximum is shown by a light dashed line, with the corresponding scale on the right-hand side of the figure. In order to get the L value from the geographical coordinates, we used the DEMETER orbital data where the L value is given for each satellite location. The reflection L shell for waves reflecting above the satellite, and the L value of the LHR maximum on the raypath were recalculated using the following approximation:

$$L_{\mathrm{refl}} = L_{\mathrm{DEM}}(Re + h_{\mathrm{refl}})/(Re + h_{\mathrm{DEM}}),$$

where h_{DEM} is the altitude of DEMETER, h_{refl} is the altitude of the wave reflection, Re is the Earth's radius, and L_{DEM} is the L value of DEMETER at the latitude of the reflection in the orbital data file. A similar formula was used to relate the L shell and the altitude of the LHR maximum displayed by the grey shaded line in Figure 10.

[19] Comparison of the patterns in Figures 7 and 10 obtained with different models of geomagnetic field and plasma distribution shows their qualitative similarity along with certain quantitative differences. First of all, the ray tracing based on the plasma parameters and geomagnetic field relevant to the observations gives the dependence of the lower cutoff frequency $f1$ on the L shell, which is much closer to the measurements than that obtained from the simplified model. Therefore, these results support our sug-

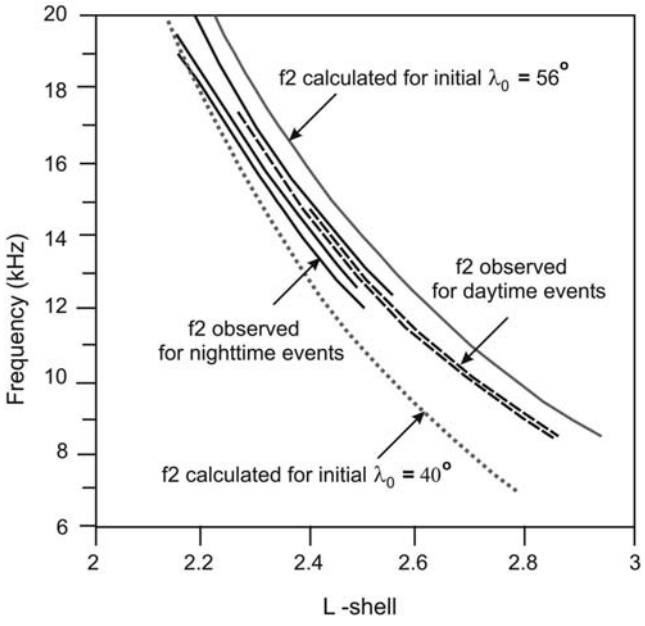


Figure 8. Upper cutoff frequency of WLE versus L shell for various WLEs.

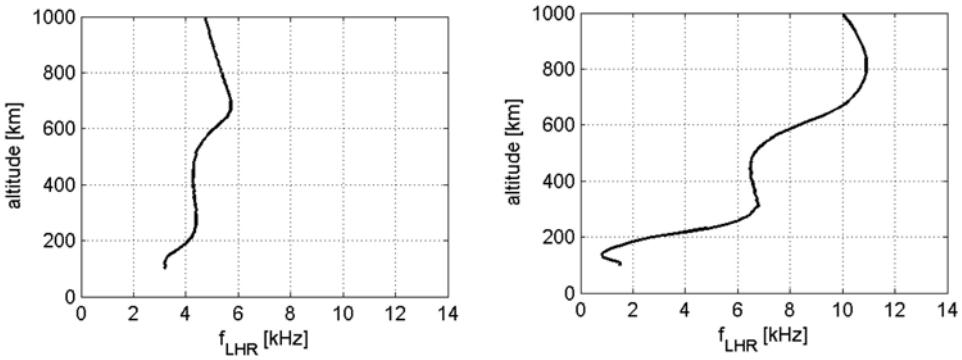


Figure 9. Typical LHR frequency profiles for (left) day and (right) night.

gestion that the LHR reflection which takes place above the satellite plays the dominant role in the formation of the lower cutoff.

[20] Finally, we present a simulated spectrogram which is expected to be the model counterpart of the overview spectrogram shown in Figure 1. The method of modeling the spectrograms related to lightning-induced emissions is described in detail by *Shklyar and Jiříček* [2000], *Shklyar et al.* [2004], and *Shklyar* [2005]. The latitude in degrees displayed on the *x* axis in Figure 11 corresponds to values on the spectrogram shown in Figure 1. The altitude and the *L*-shell variation used in simulations match the values along the corresponding orbit (shown in the figure representing the real spectrogram). Despite the apparent differences between the real and simulated spectrogram, the latter reveals many important features of the former, namely: (1) a quite accurate reproduction of the upper frequency cutoff; (2) a significant increase of the dispersion and spectral intensity near the upper cutoff frequency, which appear to be common properties; and (3) the existence of the lower cutoff frequency, although it is quantitatively different in simulations and on the real spectrogram.

[21] We obtained similar results for the simulation of WLE along the parts of orbits where the satellite moves toward lower *L* shells (see Figure 4 for an example of the real spectrogram). In these cases, the simulated upper cutoff frequency *f*2 increases along the orbit in a good agreement with observations, however, the lower cutoff frequency *f*1 exhibits larger discrepancy with real measurements. Note that the simulation of an overview spectrogram requires calculations of trajectories and all wave parameters, including the variation of the ray tube cross sections, for many

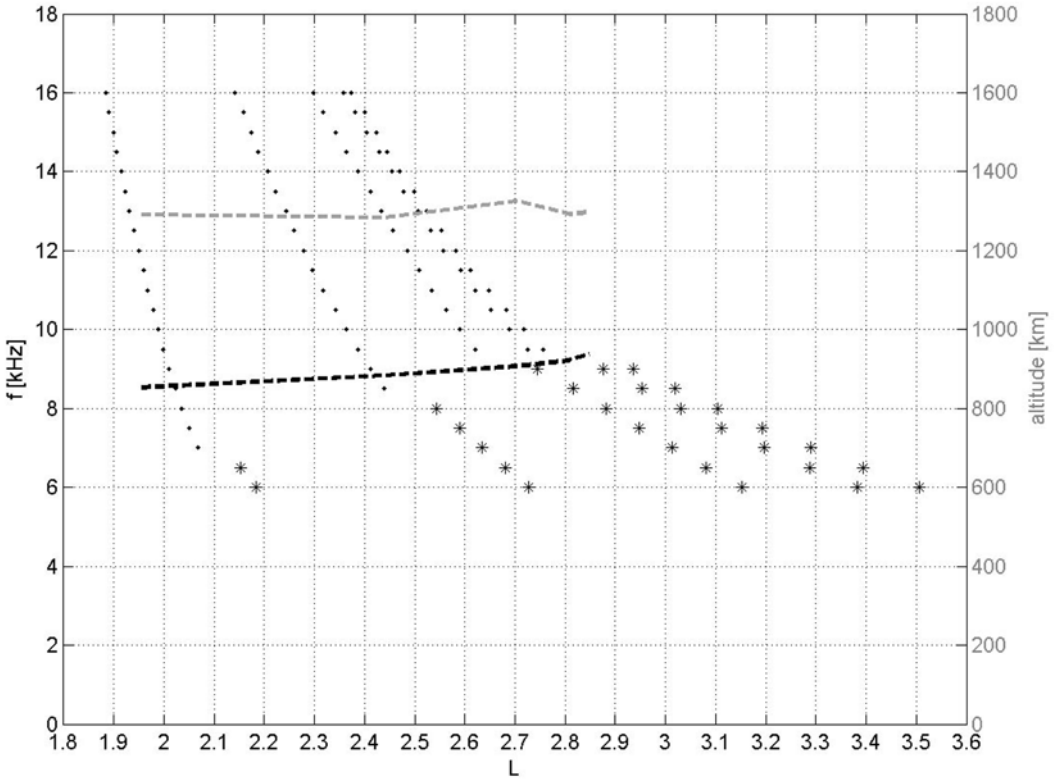


Figure 10. (*L* – *f*) plane defining expected frequency cutoffs calculated with plasma parameters appropriate to the spectrogram in Figure 1.

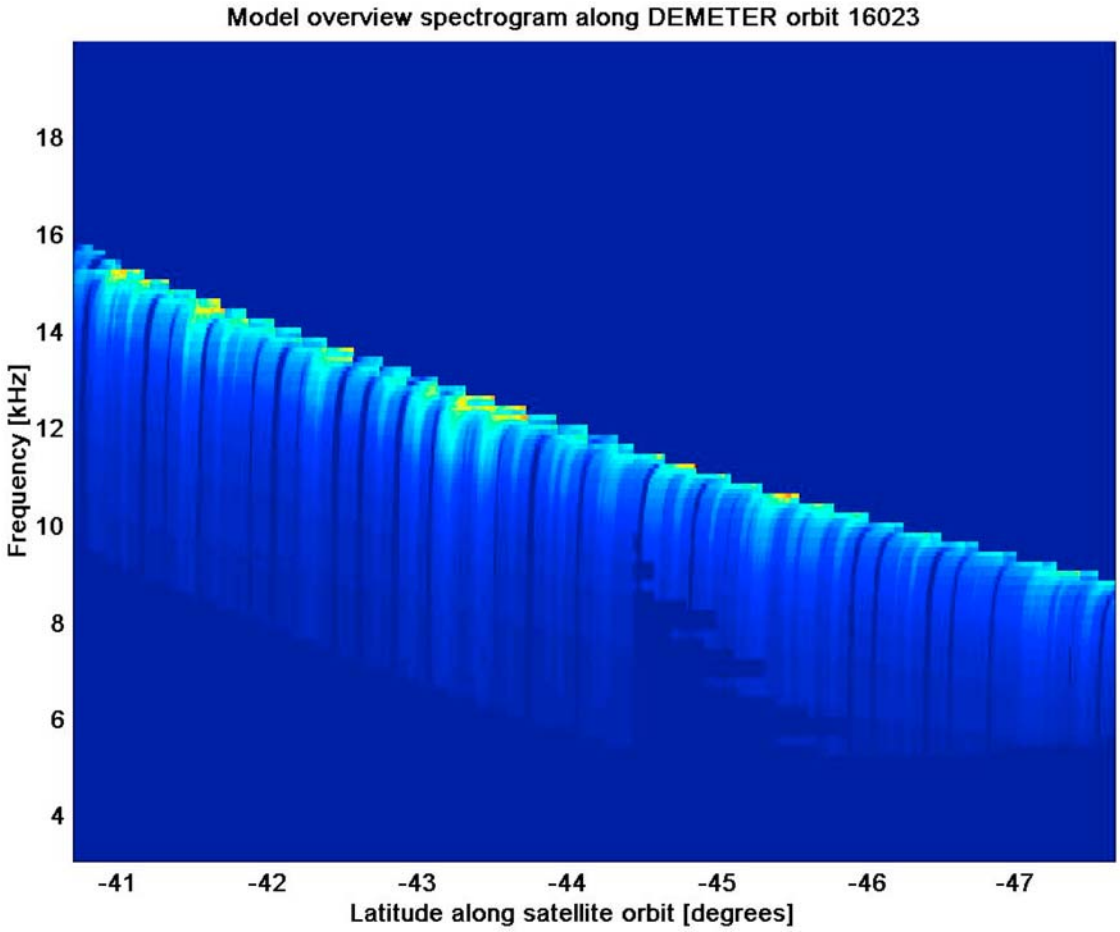


Figure 11. Simulated spectrogram typical of a poleward part of the orbit.

thousands of rays. That is why the simulations have been performed using simplified (purely analytical) models of the geomagnetic field, plasma density distribution, and the LHR frequency.

[22] As follows from the present work, the events, which have the wedge-like shape on overview spectrograms, consist of a series of "walking-trace" whistlers described and explained qualitatively by *Walter and Angerami* [1969]. Our work provides confirmation, further development, and application of their ideas to the data from the DEMETER satellite. Apart from the first time observations of pure WLE, new theoretical points include quantitative description of the upper frequency cutoff, and explanation of diurnal dependence of the lower frequency cutoff.

4. Summary

[23] The LHR frequency is known to play a crucial role in VLF wave propagation in the plasmasphere, in particular, quasiresonance VLF waves cannot propagate in a region where the LHR frequency exceeds the wave frequency. When such a wave propagates in the direction of increasing LHR frequency, it is reflected at the level where its frequency is close to the local LHR frequency. The intensity of quasiresonance waves significantly increases close to LHR frequency due to substantial decrease of the group velocity. As a consequence, the LHR associated phenomena are among the most pronounced in the VLF measurements on satellites. This concerns, first of all, electric field measurements because of the quasi-electrostatic nature of resonance LHR waves. In this respect DEMETER is of particular value as it is orbiting in the region of the upper ionosphere where the height profile of the LHR frequency forms a trough, so that the maximum of LHR frequency along the geomagnetic field line is above the satellite. The VLF phenomena presented in this paper, i.e., the formation of a wedge-like structures on overview spectrograms, are explained in terms of the wave propagation features and a specific position of the satellite with respect to the LHR maximum. In general terms, this explanation, which is in line with the analysis of *Walter and Angerami* [1969], consists of the following. WLE is formed by whistler-mode waves originating from lightnings and thus is related to thunderstorm activity. The wedge as such is formed by whistler waves propagating in a quasiresonance regime. All quasiresonance waves with frequencies below the LHR maximum are reflected above the satellite, which explains the lower frequency cutoff of the WLE, which is thus close to the maximum of the LHR frequency above the satellite. The appearance of an upper cutoff frequency is due to another feature of unducted VLF wave propagation, which consists in the trajectory merging into a limiting trajectory for waves with the same frequency, but starting from different latitudes in the opposite hemi-

sphere. As the further increase of the initial latitude does not lead to an increase of the final L shell in the opposite hemisphere, there appears a maximum L shell on which the waves with the given frequency can be observed. This L shell decreases with the increase of wave frequency due to a more pronounced bending toward lower L shells for higher-frequency waves. As a result, the accessible domain for quasiresonance whistler-mode waves on the ($L - f$) plane takes the observed wedge-like shape.

[24] **Acknowledgments.** This work was supported by the Centre National d'Etudes Spatiales (CNES). It is based on the electric field measurements in the frame of the ICE experiment on board DEMETER. The authors thank J. J. Berthelier for providing the data on the electric field. The PICS grant 3725 from CNRS/DREI, CNRS-RFBR grant 06-02-72560a, and LAPBIAT-2 Project RITA-CT-2006-025969 are also acknowledged, as well, as are programs M100420902 and M100420903 of the international cooperation of the Academy of Sciences of the Czech Republic, KONTAKT project ME09107 of the Ministry of Education, and grant 205/09/1253 of the Grant Agency of the Czech Republic.

[25] Amitava Bhattacharjee thanks David Lauben and another reviewer for their assistance in evaluating this manuscript.

References

Alekhin, Y. K., and D. R. Shklyar (1980), Some questions of electromagnetic wave propagation in magnetosphere, *Geomag. Aeron.*, *20*, 501–507.

Berthelier, J. J., et al. (2006a), ICE, the electric field experiment on DEMETER, *Planet. Space Sci.*, *54*, 456–471, doi:10.1016/j.pss.2005.10.016.

Berthelier, J. J., et al. (2006b), IAP, the thermal plasma analyzer on DEMETER, *Planet. Space Sci.*, *54*, 487–501.

Bortnik, J., U. S. Inan, and T. F. Bell (2003a), Frequency-time spectra of magnetospherically reflecting whistlers in the plasmasphere, *J. Geophys. Res.*, *108*(A1), 1030, doi:10.1029/2002JA009387.

Bortnik, J., U. S. Inan, and T. F. Bell (2003b), Energy distribution and lifetime of magnetospherically reflecting whistlers in the plasmasphere, *J. Geophys. Res.*, *108*(A5), 1199, doi:10.1029/2002JA009316.

Bošková, J., F. Jiříček, D. R. Shklyar, E. E. Titova, and P. Tříska (1988), LHR whistlers in the outer ionosphere as observed on satellites, *Adv. Space Res.*, *8*, 133–136.

Bošková, J., F. Jiříček, P. Tříska, D. R. Shklyar, and E. E. Titova (1990a), *LHR whistlers, Stud. Geophys. Geod.*, *34*, 137–146.

Bošková, J., F. Jiříček, B. V. Lundin, D. R. Shklyar, and P. Tříska (1990b), A possible common nature of equatorial half-gyrofrequency VLF emissions and discrete plasmaspheric emissions, *Ann. Geophys.*, *8*, 755–764.

Cairo, L., and F. Lefeuvre (1986), Localization of sources of ELF/VLF hiss observed in the magnetosphere: Three-dimensional ray tracing, *J. Geophys. Res.*, *91*, 4352–4364, doi:10.1029/JA091iA04p04352.

Cerisier, J. (1970), Propagation perpendiculaire au voisinage de la frequence de la resonance hybride basse, in *Plasma Waves in Space and in the Laboratory*, vol. 2, pp. 487–521, Edinburgh Univ. Press, Edinburgh, U.K.

Chum, J., F. Jiříček, and D. R. Shklyar (2003), Oblique noise bands above local LHR frequency, *Adv. Space Res.*, *31*(5), 1253–1258.

Chum, J., O. Santolik, and M. Parrot (2009), Analysis of subprotonospheric whistlers observed by DEMETER: A case study, *J. Geophys. Res.*, *114*, A02307, doi:10.1029/2008JA013585.

Edgar, B. C. (1976), The upper- and lower-frequency cutoffs of magnetospherically reflected whistlers, *J. Geophys. Res.*, *81*, 205–211.

Fišer, J., J. Chum, G. Diendorfer, M. Parrot, and O. Santolik (2010), Whistler intensities above thunderstorms, *Ann. Geophys.*, *28*, 37–46.

Gendrin, R. (1961), Le guidage des whistlers par le champ megnetique, *Planet. Space Sci.*, *5*, 274–282.

Ginzburg, V. L., and A. A. Rukhadze (1972), Waves in magnetoactive plasma, in *Handbuch der Physik*, vol. 49, Part IV, edited by S. Flügge, p. 395, Springer, Berlin.

Helliwell, R. A. (1965), Whistlers and Related Ionospheric Phenomena, Stanford Univ. Press, Stanford, Calif.

Inan, U. S., H. C. Chang, R. A. Helliwell, W. L. Imhof, J. B. Reagan, and M. Walt (1985), Precipitation of radiation belt electrons by man-made waves: A comparison between theory and measurement, *J. Geophys. Res.*, *90*, 359–369.

Jiříček, F., and D. R. Shklyar (1999), On the problem of quasi-resonance wave trapping in LHR waveguide, *Geomag. Aeron. Int.*, *1*, 193–201.

Kimura, I. (1966), Effects of ions on whistler-mode ray tracing, *Radio Sci.*, *1*, 269–283.

Kimura, I. (1985), Whistler mode propagation in the Earth and planetary magnetospheres and ray tracing techniques, *Space Sci. Rev.*, *42*, 449–466.

Lauben, D. S., U. S. Inan, and T. F. Bell (2001), Precipitation of radiation belt electrons induced by obliquely propagating lightning generated whistlers, *J. Geophys. Res.*, *106*, 29,745–29,770.

Parrot, M. (Ed.) (2006), Special Issue: First results of the DEMETER micro-satellite, *Planet. Space Sci.*, *54*, pp. 411–557.

Parrot, M., et al. (2006), The magnetic field experiment IMSC and its data processing onboard DEMETER: Scientific objectives, description and first results, *Planet. Space Sci.*, *54*, 441–455, doi:10.1016/j.pss.2005.10.015.

Parrot, M., J. J. Berthelier, J. P. Lebreton, R. Treumann, and J. L. Rauch (2008), DEMETER observations of EM emissions related to thunderstorms, *Space Sci. Rev.*, *137*, 511–519, doi:10.1007/s11214-0089347-y.

Santolik, O., M. Parrot, and F. Lefeuvre (2003), Singular value decomposition methods for wave propagation analysis, *Radio Sci.*, *38*(1), 1010, doi:10.1029/2000RS002523.

Santolik, O., M. Parrot, U. S. Inan, D. Buresova, D. A. Gurnett, and J. Chum (2009), Propagation of unducted whistlers from their source lightning: A case study, *J. Geophys. Res.*, *114*, A03212, doi:10.1029/2008JA013776.

Shklyar, D. R., and F. Jiříček (2000), Simulation of nonducted whistler spectrograms observed aboard the MAGION 4 and 5 satellites, *J. Atmos. Sol. Terr. Phys.*, *62*, 347–370.

Shklyar, D. R. (2005), Key problems in numerical simulation of spectrograms related to emissions caused by lightning strokes, *Geomagnetism and Aeronomy*, *45*, 474–487.

Shklyar, D. R., J. Chum, and F. Jiříček (2004), Characteristic properties of Nu whistlers as inferred from observations and numerical modelling, *Ann. Geophys.*, *22*, 3589–3606.

Smith, R. L., and J. J. Angerami (1968), Magnetospheric properties deduced from OGO 1 observations of ducted and nonducted whistlers, *J. Geophys. Res.*, *73*, 1–20.

Smith, R. L., and N. M. Brice (1964), Propagation in multicomponent plasmas, *J. Geophys. Res.*, *69*, 5029–5040.

Smith, R. L., I. Kimura, J. Vineron, and J. Katsufrakis (1966), Lower hybrid resonance noise and a new ionospheric duct, *J. Geophys. Res.*, *71*, 1925–1927.

Sonwalkar, V. S., U. S. Inan, T. F. Bell, R. A. Helliwell, V. M. Chmyrev, Y. P. Sobolev, O. Y. Ovcharenko, and V. Selegej (1994), Simultaneous observations of VLF ground transmitter signals on the DE 1 and COSMOS 1809 satellites: Detection of a magnetospheric caustic and a duct, *J. Geophys. Res.*, *99*, 17,511–17,522.

Sonwalkar, V. S., A. Reddy, D. L. Carpenter, and B. W. Reinisch (2008), Whistler mode sounding of the magnetosphere: Measurement of electron density, ion composition (H^+, HE^+, O^+), and density irregularities along the geomagnetic field, paper presented at the 29th General Assembly, URSI, Chicago, Ill., 7–16 Aug.

Storey, L. R. O. (1953), An investigation of whistling atmospherics, *Phil. Trans. R. Soc. London, Ser. A*, *246*, 113–141.

Triskova, L., V. Truhlik, and J. Smilauer (2003), An empirical model of ion composition in the outer ionosphere, *Adv. Space Res.*, *31*, 653–663.

Triskova, L., V. Truhlik, and J. Smilauer (2006), An empirical topside electron density model for calculation of absolute ion densities in IRI, *Adv. Space Res.*, *37*, 928–934.

Truhlik, V., L. Triskova, and J. Smilauer (2004), New advances in empirical modelling of ion composition in the outer ionosphere, *Adv. Space Res.*, *33*, 844–849.

Walker, A. D. M. (1976), The theory of whistler propagation, *Rev. Geophys.*, *14*, 629–638.

Walter, F., and J. J. Angerami (1969), Nonducted mode of VLF propagation between conjugate hemispheres; observations on OGO's 2 and 4 of the "walking-trace" whistler and of Doppler shifts in fixed frequency transmissions, *J. Geophys. Res.*, *74*, 6352–6370.

Yabroff, I. (1961), Computation of whistler ray paths, *J. Res. NBS*, *65D*, 485–505.

J. Chum and O. Santolik, Institute of Atmospheric Physics AS CR, Bocni II/1401, 14131 Praha 4, Czech Republic. (jachu@ufa.cas.cz; ondrej.santolik@mff.cuni.cz)

M. Parrot, LPC2E/CNRS, 3A Avenue de la Recherche Scientifique, F-45071 Orléans CEDEX 2, France. (mparrot@cnrs-orleans.fr)

D. R. Shklyar, Space Research Institute, Russian Academy of Sciences, Profsoyuznaya str. 84/32, 117997 Moscow, Russia. (david@iki.rssi.ru)

E. E. Titova, Polar Geophysical Institute, Apatity, Murmansk, Russia. (lena.titova@gmail.com)